AIP | The Journal of Chemical Physics

Anharmonic state counts and partition functions for molecules via classical phase space integrals in curvilinear coordinates

Eugene Kamarchik and Ahren W. Jasper

Citation: J. Chem. Phys. **138**, 194109 (2013); doi: 10.1063/1.4804420
View online: http://dx.doi.org/10.1063/1.4804420
View Table of Contents: http://jcp.aip.org/resource/1/JCPSA6/v138/i19
Published by the American Institute of Physics.

Anharmonic state counts and partition functions for molecules via classical phase space integrals in curvilinear coordinates

Eugene Kamarchik[a] and Ahren W. Jasper[b]
Combustion Research Facility, Sandia National Laboratories, Livermore, California 94551, USA

(Received 12 February 2013; accepted 26 April 2013; published online 21 May 2013)

An algorithm is presented for calculating fully anharmonic vibrational state counts, state densities, and partition functions for molecules using Monte Carlo integration of classical phase space. The algorithm includes numerical evaluations of the elements of the Jacobian and is general enough to allow for sampling in arbitrary curvilinear or rectilinear coordinate systems. Invariance to the choice of coordinate system is demonstrated for vibrational state densities of methane, where we find comparable sampling efficiency when using curvilinear z-matrix and rectilinear Cartesian normal mode coordinates. In agreement with past work, we find that anharmonicity increases the vibrational state density of methane by a factor of ∼2 at its dissociation threshold. For the vinyl radical, we find a significant (∼10×) improvement in sampling efficiency when using curvilinear z-matrix coordinates relative to Cartesian normal mode coordinates. We attribute this improved efficiency, in part, to a more natural curvilinear coordinate description of the double well associated with the H_2C–C–H wagging motion. The anharmonicity correction for the vinyl radical state density is ∼1.4 at its dissociation threshold. Finally, we demonstrate that with trivial parallelizations of the Monte Carlo step, tractable calculations can be made for the vinyl radical using direct *ab initio* potential energy surface evaluations and a composite QCISD(T)/MP2 method. © *2013 AIP Publishing LLC*. [http://dx.doi.org/10.1063/1.4804420]

I. INTRODUCTION

Accurate bimolecular or unimolecular transition state theory (TST) calculations require accurate partition functions and state counts for the reactant and the transition state species. However, the quantum mechanical harmonic oscillator (HO) approximation is often used in practical applications of TST as it greatly simplifies the evaluation of the partition functions and state counts. This approximation has two parts. First, each vibrational mode is assumed to be uncoupled from the other vibrational modes and from rotations, and, second, each vibration is assumed to take place on a quadratic potential energy surface. Despite the apparent severity of these assumptions, the HO approximation has been widely applied and found to be of enormous practical utility in both kinetics and thermochemistry. In fact, only fairly recently has the uncertainty in calculated values of the reaction barrier, $V^{\ddagger}$, for molecular systems been reduced enough to compete with the uncertainty arising from the HO approximation. With values of $V^{\ddagger}$ now routinely calculated with "chemical accuracy,"[1] the HO approximation can be the dominant source of uncertainty in calculations of the rate constant, particularly at elevated temperatures where tunneling is not expected to be important and where the exponential mitigates the uncertainty associated with $V^{\ddagger}$.[2]

Numerous methods have been proposed for calculating anharmonic state counts and partition functions. Torsions are often treated as a special kind of vibration and may be approximated as separable (uncoupled) from the other vibrations and as a collection of independent one-dimensional hindered rotors.[3–5] Similar methods may be applied for other kinds of one-dimensional anharmonicities (e.g., Morse oscillators, squarer-than-quadratic bends, etc.). When anharmonic coupling is neglected, the total partition function is the product of the one-dimensional ones, and the total number of states is readily calculated via direct quantum mechanical state counts[6,7] or classical convolutions.[4] Pitzer and Gwinn[8] proposed an ambitious treatment of coupled torsions 70 years ago, but this method has not found widespread use. A recently developed method for treating torsions that include some anharmonic coupling is the multi-structural approximation of Truhlar and co-workers,[9] which is applicable to molecular systems and includes the effect of the change in local mode frequencies due to torsional conformer changes. We refer the reader to the introduction of Ref. 9 for a recent summary of other methods that have been proposed for treating torsions. Although these specialized methods for torsions may be practically useful, they typically involve the separable approximation for the torsions mentioned above and *ad hoc* models to approximate some of the missing anharmonic couplings. It is difficult to appraise their predictive accuracy as there have been few comparisons of these treatments with higher-level methods[10,11] and none for systems larger than a few atoms.

Direct quantum mechanical state counts based on either the exact or approximate solution of the rovibrational Hamiltonian[12–15] may be performed. However, these methods are limited to small systems and, even when such calculations are possible, it is difficult to obtain spectra up to high enough energies to converge the calculated kinetics and/or thermochemistry at moderate and high temperatures.

[a]Electronic mail: ekamarc@sandia.gov
[b]Electronic mail: ajasper@sandia.gov

Nguyen and Barker implemented and validated a practical approach for calculating anharmonic state counts and partition functions, including anharmonic coupling, for molecular systems.[16,17] Their method is based on a spectroscopic expansion of the potential energy surface, requires readily computed local information near the potential energy surface minimum, and was shown to be very accurate when compared with accurate quantum mechanical state counts for small systems. This method may be systematically more accurate than the HO approximation for local vibrations but is similarly not applicable to nonlocal motions such as torsions. Furthermore, the spectroscopic expansion has known deficiencies relating to "turnover" where the energy artificially decreases with increasing vibrational quantum number at high energy due to the truncated expansion.

Troe and Ushakov have described a series of detailed semiempirical corrections to the HO approximation,[18] and these were extended and evaluated by Schmatz for large systems.[19] These corrections may be readily applied, even to very large systems, but their predictive accuracy is unknown.

Finally, we consider the evaluation of state counts and partition functions via classical Monte Carlo phase space integration.[20–23] Phase space integration has the significant advantages that it is generally applicable, it does not require an expansion about a preferred potential energy minimum and so can naturally treat nonlocal vibrations, and it is (classically) exact, including both single-mode anharmonicity and anharmonic coupling. This approach may be readily applied to calculate transition state properties, although such applications remain rare and have been limited to small systems.[24–26] The resulting classical partition functions can be quantum-corrected via Pitzer and Gwinn's "useful approximation,"[8]

$$Q_q \approx Q_c \frac{Q_q^{HO}}{Q_c^{HO}}, \tag{1}$$

or Doll's analog for the state count, W,[24] where the superscript "HO" denotes the harmonic approximation and the subscripts "q" and "c" denote quantum mechanical and classical partition functions, respectively. Alternatively, classical state counts may be corrected via semiclassical rules, such as the Whitten-Rabinovich approximation[27] or obtained via the inverse Laplace transform.[28] Finally, we note that exact quantum mechanical partition functions can be obtained when this approach is coupled with path integral methods.[29–31] Classical Monte Carlo phase space integration is particularly well-suited for high-temperature/high-energy applications, where the number of states is large and quantum effects are not as important.

Here we implement Monte Carlo phase space integration in arbitrary curvilinear or rectilinear coordinates with numerical evaluations of the volume element. Whereas previous implementations have used Cartesian normal mode coordinates or specialized coordinates for small systems, the present approach allows for more straightforward application to larger systems and to systems with nonlocal motions. Recently, the realization that optimized coordinate systems can result in reduced potential energy and kinematic couplings, particularly for large displacements, has lead to their use in vibrational calculations.[32–34] Thus, we expect that, the use of curvilinear coordinates can result in more efficient sampling for some systems and allow for more natural reduced-dimensional calculations.

Theoretical details of our implementation are given in Sec. II. In Sec. III, calculated values of the density of states, ρ, and the partition function, Q, for methane are used to demonstrate the method's invariance with respect to the choice of coordinate system. An application to a system with nonlocal motions is also made. State densities for the vinyl radical, which features a nonlocal double well for the H_2C–C–H wagging motion, are calculated to demonstrate the improved efficiency of using z-matrix coordinates for this system. This system is also used to demonstrate that efficient Monte Carlo phase space integration calculations can be performed, even with direct evaluations of an accurate *ab initio* potential energy surface.

II. THEORY

Classically, the number of vibrational states in an α-dimensional system with energy less than or equal to E, $W(E)$, and subject to the constraint of zero total angular momentum ($J = 0$) is given by the integral over phase space,

$$W(E) = h^{-\alpha} \int u[E - H(\mathbf{x}, \mathbf{p})]\, d\mathbf{x}\, d\mathbf{p}, \tag{2}$$

where $\mathbf{x}$ are the Cartesian coordinates, $\mathbf{p}$ the conjugate momenta, and u is the Heaviside step function making the integral only non-zero over the space such that the Hamiltonian $H(\mathbf{x}, \mathbf{p})$ has energy less than or equal to E. Similarly, the rovibrational density of states is given by

$$W(E) = h^{-(\alpha+3)} \int u[E - H(\mathbf{x}, \mathbf{p}, \mathbf{j})]\, d\mathbf{x} \sin\theta\, d\theta\, d\psi\, d\phi\, d\mathbf{p}\, d\mathbf{j}, \tag{3}$$

where θ, ψ, and ϕ are the three Euler angles (which are omitted from the Hamiltonian, since neither the potential energy nor the kinetic energy depends on them), and $\mathbf{j}$ are the three components of the angular momentum. Despite their relatively simple forms, direct evaluation of these integrals is complicated by three problems: (i) it is a high-dimensional integral (either $6N - 12$ for the purely vibrational space or $6N - 6$ for the rovibrational space, where N is the number of atoms), (ii) the sampling domain should contain the entire set of coordinates for which $H \leq E$, but this domain is not generally known, and (iii) the Hamiltonian operator must be efficiently evaluated. The high-dimensionality of the problem effectively rules out direct numerical integration via standard grid-based quadrature rules while the complexity of the underlying potential energy surface appearing in the Hamiltonian also effectively prohibits analytic evaluation. Monte Carlo integration is possible provided that the challenges associated with (ii) and (iii) can be overcome.

We first turn our attention to the former problem of specifying an appropriate sampling domain. The domain where the integrand is nonzero corresponds to the condition, $H \leq E$, but the shape of this domain is not known. We instead define a sampling domain that is more convenient to specify and that includes the $H \leq E$ region. Momenta are not

sampled, and this part of the integral is handled analytically, as discussed below. Coordinates are sampled in a hyperrectangle with edges defined by minimum and maximum values of the chosen coordinates. While any set of coordinates can allow all possible configurations with $H \leq E$ to be sampled, the choice of coordinates greatly affects the efficiency of evaluating the integral in Eq. (2) by Monte Carlo integration. Indeed, poor choices of coordinates can result in sampling domains with negligible fractions corresponding to $H \leq E$, particularly for large molecules, where an optimum or near-optimum set of coordinates is required. For better choices of the coordinates, the sampling domain more closely approximates geometries where $H \leq E$ and thus there are fewer wasted samplings. Other authors have employed different schemes for specifying non-rectangular coordinate bounds[17] or used Jacobi coordinates for three-atom systems.[20] In this work we will consider two natural choices for the coordinate system, namely, displacements along mass-weighted Cartesian normal modes and chemist's or z-matrix (bond length, bond angle, dihedral coordinates). The algorithm we present, however, is constructed in such a way that it can be applied to any choice of rectilinear or curvilinear coordinate system.

The integral in Eqs. (2) and (3) can be simplified by starting from the expression for the Hamiltonian in Cartesian coordinates,

$$H(\mathbf{x}, \mathbf{p}, \mathbf{j}) = \sum_{i=1}^{\alpha} \frac{1}{2m_i} p_i^2 + \sum_{i=1}^{3} \frac{1}{2I_i} j_i^2 + V(\mathbf{x}), \tag{4}$$

where I_i is the moment of inertia associated with the three rotational degrees of freedom. Coupling terms between rotational and vibrational coordinates are omitted because we assume the separation between these degrees of freedom is carried at a geometry given by $\mathbf{x}$, for which it is exact. In mass-weighted Cartesian normal coordinates, all of the reduced masses associated with the vibrational degrees of freedom are in unity, and then the integral over the momenta can be carried out analytically, yielding the expression for the $J = 0$ case of

$$W(E) = h^{-\alpha} \int u[E - H(\mathbf{x}, \mathbf{p})] S^{\alpha}(p(\mathbf{x})) d\mathbf{x}, \tag{5}$$

or, for the rovibrational case,

$$W(E) = 8\pi^2 h^{-(\alpha+3)} \int u[E - H(\mathbf{x}, \mathbf{p}, \mathbf{j})] \times \sqrt{I_1(\mathbf{x}) I_2(\mathbf{x}) I_3(\mathbf{x})} S^{\alpha+3}(p(\mathbf{x})) d\mathbf{x}, \tag{6}$$

where S^{α} is the volume of an (α)-dimensional hypersphere with radius $p(\mathbf{x}) = \sqrt{2(E - V(\mathbf{x}))}$. Hereafter, we will primarily consider the $J = 0$ case, but all equations have analogous nonzero J versions.

While the Cartesian normal modes were useful for carrying out the integration over the momenta, we would like to be able to sample the configuration space of the molecule using an arbitrary set of coordinates, $\mathbf{q}$. The transformation of coordinates between the mass-weighted Cartesians, $\mathbf{x}$, and the arbitrary set, $\mathbf{q}$, introduces the determinant of the Jacobian,

$$J = \begin{bmatrix} \frac{\partial x_1}{\partial q_1} & \cdots & \frac{\partial x_1}{\partial q_\alpha} \\ \vdots & \ddots & \vdots \\ \frac{\partial x_{3N}}{\partial q_1} & \cdots & \frac{\partial x_{3N}}{\partial q_\alpha} \end{bmatrix}, \tag{7}$$

as an additional factor in the integral. After this transformation, we have, as our final working equation for the integration,

$$W(E) = h^{-\alpha} \int u[E - H(\mathbf{q}, \mathbf{p})] |J(\mathbf{q})| S^{\alpha}(p(\mathbf{q})) d\mathbf{q}, \tag{8}$$

or a similar expression for the rovibrational case.

Rather than attempt to derive analytic Jacobians for arbitrary choices of $\mathbf{q}$, we adopt the following numerical procedure. To begin, we define transformations that convert from our choice of arbitrary coordinates, $\mathbf{q}$, to body-fixed mass-weighted Cartesian coordinates, $\mathbf{x}$, having their origin at the center-of-mass. The partial derivatives are calculated numerically as

$$\frac{\partial x_i}{\partial q_j} = \frac{x_i(q_1, \ldots, q_j - h, \ldots, q_\alpha) - x_i(q_1, \ldots, q_j + h, \ldots, q_\alpha)}{2h}. \tag{9}$$

From this procedure we construct the $3N \times 3N - 6$ ($3N \times 3N - 3$ for nonzero J) deformation matrix,

$$D = \begin{bmatrix} \frac{\partial x_1}{\partial q_1} & \cdots & \frac{\partial x_1}{\partial q_{3N-6}} \\ \vdots & \ddots & \vdots \\ \frac{\partial x_{3N}}{\partial q_1} & \cdots & \frac{\partial x_{3N}}{\partial q_{3N-6}} \end{bmatrix}, \tag{10}$$

from which we can evaluate the determinant of the Jacobian as $|J(\mathbf{q})| = \sqrt{|D^T D|}$. This scheme is similar to one that has been employed in vibrational structure and quantum dynamics to numerically construct Wilson's G matrix and evaluate the kinetic energy operator.[35,36]

In Monte Carlo integration, random configurations are chosen within a uniformly sampled domain and the integral is evaluated as

$$\int_{\Omega} f(\mathbf{y}) d\mathbf{y} \approx \frac{\Omega}{M} \sum_{i=1}^{M} f(\mathbf{y}), \tag{11}$$

where Ω denotes the total volume of the sampled region and $\mathbf{y}$ is a uniformly sampled variate. In our case, the integral for W becomes

$$W(E) = \frac{\Omega(\Delta q)}{M h^{\alpha}} \sum_{i=1}^{M} F(\mathbf{q}_i), \tag{12}$$

where $F(\mathbf{q_i})$ is equal to the integrand of Eq. (8) evaluated at $\mathbf{q_i}$ and M is the number of samples. The domain of integration is given by the hyperrectangle $\{\Delta q | a_1 \leq q_1 \leq b_1, \ldots, a_\alpha \leq q_\alpha \leq b_\alpha\}$, which yields the final expression,

$$\Omega(\Delta q) = \frac{\prod_{i=1}^{\alpha}(b_i - a_i)}{M} \sum_{i=1}^{M} |J(\mathbf{q}_i)|. \tag{13}$$

The boundaries of the hyperrectangle could be chosen in a variety of ways and will affect the overall performance of the algorithm. The details of the strategy for choosing these bounds will be discussed later. In our implementation, W is calculated simultaneously over a range of energies. The contribution of each sampled geometry to $W(E)$ from $E = 0$ up to $E_{\max}$ is evaluated, where E_{max} is a parameter. The density of states, $\rho(E)$, is evaluated from $W(E)$ by numerical differentiation,

$$\rho(E) = \frac{W(E+\epsilon) - W(E-\epsilon)}{2\epsilon}, \tag{14}$$

with $\epsilon = 1\ \mathrm{cm}^{-1}$. While one could also evaluate $\rho(E)$ directly, by replacing the Heaviside step function with a corresponding δ-function in Eq. (8), we have found the numerical differentiation to be quite stable and to yield good results.

Above the energy for dissociation, the integral given in Eq. (8) can become unbounded since it becomes possible to extend infinitely along certain coordinates. This does not present a practical difficulty however, since we will place boundaries on the configuration space in order to limit the integral to the regions of interest. Other methods for calculating $\rho(E)$ and $W(E)$ encounter similar difficulties and must resort to similar truncations in order to confine the space. For instance, state counts based on spectroscopic expansions truncate the order of the potential to keep the space bounded, while direct counts based on solving the rovibrational Hamiltonian effectively limit the space according to the extent of the basis employed. Furthermore, we expect state counts and densities evaluated above the threshold energy with such truncations in place to nonetheless be accurate for many applications, at least for some range of energies close to threshold. At these energies, the number of quasibound states that are correctly included in the truncated state count is likely much greater than the number of continuum states that are being partially miscounted.

In the subsequent numerical tests, we define the anharmonicity corrections factors as, e.g.,

$$f(E) = \frac{\rho_A(E)}{\rho_H(E)}, \tag{15}$$

where $\rho_A(E)$ is the anharmonic density of states and $\rho_H(E)$ is the harmonic density of states. Comparison of the numerical results with the harmonic oscillator results is useful, both because it allows us to define a correction factor to the density of states and hence to the partition function and rate coefficient calculations as well as to estimate the uncertainty of the Monte Carlo procedure, since exact expressions for $\rho_H(E)$ are known. Furthermore, these corrections are of direct relevance to many conventional kinetics calculations, where the HO approximation is often employed.

III. RESULTS AND DISCUSSION

A. Methane

The main purpose of the tests involving CH_4 is to test the exactness of the numerical procedure for constructing the Jacobian as well as to check the convergence behavior of our algorithm. CH_4 is a good benchmark molecule because we can expect that both z-matrix and Cartesian normal modes will equally be the good representations of the important molecular configurations, and so we should be able to converge the results in either coordinate system with similar efficiencies. This is because methane has no low frequency normal modes and its vibrations can be well described by local motions. Additionally, we can make use of a very fast CH_4 potential based on the tight-binding model[37,38] so that we can easily achieve millions of sampled geometries and test the rate of convergence of the Monte Carlo integration.

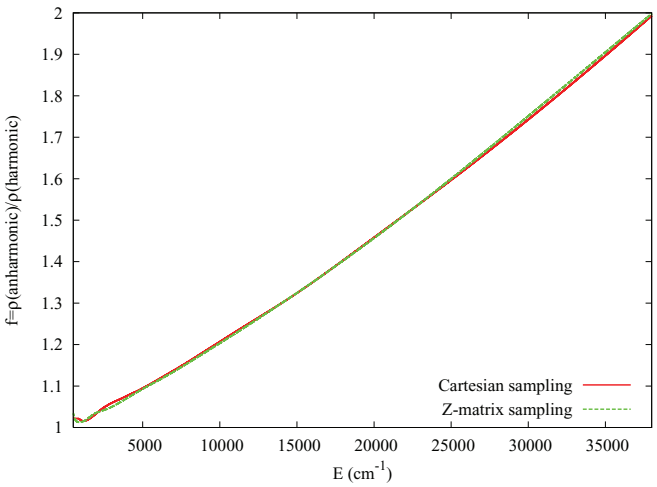

FIG. 1. Comparison of the anharmonicity correction to ρ for CH_4 computed using Cartesian normal-mode and z-matrix coordinates.

Figure 1 shows a comparison between the density of states generated for CH_4 using Cartesian normal mode sampling and z-matrix coordinates. In both cases the hyperrectangle was defined by single turning points on the real potential for $E = 30\,000\ \mathrm{cm}^{-1}$. This hyperrectangle was then divided up into a series of nested hyperrectangles and each one was sampled independently. Such a procedure can be used to effectively bias the sampling towards the lower-energy regions and reduce the statistical error in those regions, which helps to reduce the statistical error in the thermodynamic properties. As can be seen from Figure 1, the two methods generate identical state densities (plotted here as the anharmonicity correction factor for the state density). At the bond dissociation energy, the anharmonicity correction factor to W is 1.98 which agrees with the values obtained by Nguyen and Barker[17] and Schmatz.[19]

A set of 20 trials for different sample sizes between $M = 10\,000$ and $1\,000\,000$ was used to quantify the rate of convergence for both Cartesian normal mode and z-matrix coordinates, shown in Fig. 2. The standard deviation and mean of the results of these 20 trials are used to illustrate the convergence of the method. We define the relative standard deviation as the standard deviation divided by the mean, $\frac{\sigma}{\bar{W}}$, and the relative maximum error as $\frac{\max(|W_i - \bar{W}|)}{\bar{W}}$. The resulting values were fit to the form $a \cdot M^b$, where a and b are fitting parameters. Both convergence metrics for Cartesian normal mode and z-matrix coordinates are shown in Fig. 2, where Cartesian normal mode coordinates slightly outperform the z-matrix coordinates. The sampling error for both decreases as the square root of the number of samples, which is the expected result

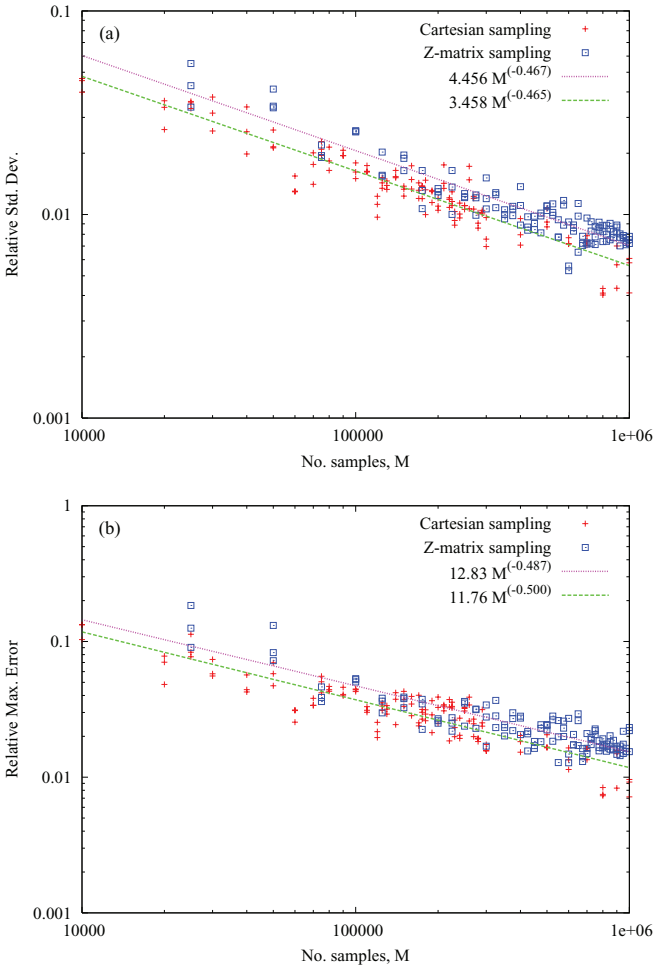

FIG. 2. (a) Relative standard deviation and (b) relative maximum error for W at three energies: 10 000 cm^{-1}, 15 000 cm^{-1}, and 20 000 cm^{-1} using both coordinate systems. Each point on the plot corresponds to the convergence metrics evaluated for one of the three energies using the specified coordinate system and for some value of M. The solid curves are the best fits of the data points to the form $a \cdot M^b$.

for Monte Carlo algorithms. Both the z-matrix and Cartesian coordinate achieve sampling uncertainties of less than 2% at fewer than 100 000 samples.

In order to further assess the accuracy of the computed anharmonicity correction factor, we have compared the partition function obtained via Eq. (1) with the $J = 0$ partition function obtained from direct calculation of the vibrational energy levels using vibrational configuration interaction (VCI). These results are shown in Table I. There is in good agreement between the Pitzer–Gwinn[8] correction partition function and the VCI results, particularly at high temperatures when the correction is non-negligible. Our results for $Q_{\mathrm{vib},J=0,\mathrm{VCI}}$ are also in reasonable agreement with previous calculations for this quantity.[39]

We also have used CH_4 as a demonstration of the rovibrational sampling algorithm to illustrate the effect of coupling between rotational and vibrational degrees of freedom. The same set of sampling parameters as the above $J = 0$ run in z-matrix coordinates was used, and the resulting density of states was used to evaluate the partition function at selected temperatures. These results are shown in Table II. For comparison, the rotational partition function corresponding to a classical rigid rotor having moments of inertia corresponding to those for the equilibrium structure of CH_4 has been used as a reference for the separable case. Classically, the rotational partition function is proportional to the moments of inertia along each axis. Thus, we may expect that as the temperature increases and structures with longer C–H bonds are sampled the rotational contribution to the overall rovibrational partition function will grow, and this is indeed the case seen in Table II. In the case of CH_4 the coupling between rotation and vibration serves to further increase the anharmonicity correction relative to the harmonic oscillator-rigid rotor approximation. The coupling of vibrations to rotations is often assumed to be negligible, and these results mostly confirm that, except at high temperatures where there starts to be appreciable deviation.

TABLE I. Comparison of vibrational partition functions obtained using the harmonic approximation, the Pitzer-Gwinn[8] corrected harmonic partition function, and VCI. Results above 1500 K are not shown for VCI because it became difficult to converge sufficient vibrational states at high enough energies to converge Q.

Temperature (K)	Q_{harmonic}	$Q_{\mathrm{corrected}}$	Q_{VCI}
100	1.000	1.002	1.000
200	1.000	1.020	1.000
300	1.002	1.033	1.004
400	1.015	1.058	1.022
500	1.050	1.107	1.067
600	1.112	1.187	1.147
700	1.208	1.304	1.266
800	1.340	1.464	1.430
900	1.514	1.675	1.647
1000	1.737	1.944	1.926
1250	2.567	2.964	2.976
1500	3.957	4.711	4.748
1750	6.217	7.635	
2000	9.820	12.43	
3000	56.79	81.26	

Finally, we note that anharmonicity corrections of the ratio, $\rho(E)/Q(T)$, are of direct relevance to low-pressure unimolecular dissociation reactions.[40,41] The corrections calculated for this ratio for CH_4 vary from 2.0 to 1.5 for $T = 300$–2000 K and E equal to the dissociation threshold. As discussed elsewhere,[42] the magnitude of this correction suggests that the neglect of vibrational anharmonicity can dominate the overall error in low-pressure unimolecular dissociation calculations.

B. Vinyl radical

The tests involving the vinyl radical are designed to demonstrate direct *ab initio* sampling using this algorithm as well as to illustrate some important effects of employing curvilinear coordinates. Calculations in this section are performed either using direct sampling of a hybrid QCISD(T)/MP2 potential, where the energy is defined as $E = E(\mathrm{MP2/cc\text{-}pVTZ}) - E(\mathrm{MP2/cc\text{-}pVDZ}) + E(\mathrm{RQCISD(T)/cc\text{-}pVDZ})$, or using a fitted potential

TABLE II. Comparison of partition functions calculated with and without the inclusion of coupling between vibrations and rotations. All partition functions are calculated classically and numbers in square brackets correspond to powers of ten. The columns, respectively, are: the purely vibrational harmonic oscillator partition function, $Q_{\text{vib,har}}$; the purely vibrational anharmonic sampled partition function, $Q_{\text{vib,anh}}$; the rovibrational partition function using the harmonic vibrations and the rigid rotor approximation, $Q_{\text{rovib,anh–rr}}$; the rovibrational partition function using the anharmonic sampled vibrations and the rigid rotor approximation, $Q_{\text{rovib,anh–rr}}$; and the rovibrational partition function computed fully using the sampling algorithm, $Q_{\text{rovib,anh}}$. The anharmonicity corrections are defined as $f_{\text{vib}} = Q_{\text{vib,anh}}/Q_{\text{vib,har}}$, $f_{\text{rot}} = Q_{\text{rovib,anh}}/Q_{\text{rovib,anh–rr}}$, and $f_{\text{rovib}} = Q_{\text{rovib,anh}}/Q_{\text{rovib,har–rr}}$.

Temperature (K)	$Q_{\text{vib,har}}$	$Q_{\text{vib,anh}}$	$Q_{\text{rovib,har–rr}}$	$Q_{\text{rovib,anh–rr}}$	$Q_{\text{rovib,anh}}$	f_{vib}	f_{rot}	f_{rovib}
100	6.89[−9]	6.89[−9]	5.90[−7]	5.90[−7]	5.88[−7]	1.00	1.00	1.00
200	3.53[−6]	3.52[−6]	8.55[−4]	8.53[−4]	8.75[−4]	1.00	1.02	1.02
300	1.36[−4]	1.38[−4]	6.03[−2]	6.14[−2]	6.29[−2]	1.02	1.03	1.04
400	1.81[−3]	1.87[−3]	1.24[0]	1.28[0]	1.31[0]	1.04	1.02	1.06
500	1.35[−2]	1.42[−2]	1.29[1]	1.36[1]	1.39[1]	1.06	1.02	1.08
600	6.95[−2]	7.44[−2]	8.74[1]	9.36[1]	9.57[1]	1.07	1.02	1.10
700	2.78[−1]	3.02[−1]	4.41[2]	4.79[2]	4.90[2]	1.09	1.03	1.11
800	9.25[−1]	1.02[0]	1.79[3]	1.97[3]	2.03[3]	1.10	1.03	1.13
900	2.67[0]	2.97[0]	6.17[3]	6.86[3]	7.09[3]	1.11	1.03	1.15
1000	6.89[0]	7.75[0]	1.87[4]	2.10[4]	2.18[4]	1.12	1.04	1.17
1250	5.14[1]	5.94[1]	1.94[5]	2.25[5]	2.36[5]	1.16	1.05	1.21
1500	2.65[2]	3.16[2]	1.32[6]	1.57[6]	1.66[6]	1.19	1.06	1.26
1750	1.06[3]	1.30[3]	6.65[6]	8.16[6]	8.73[6]	1.23	1.07	1.31
2000	3.53[3]	4.46[3]	2.70[7]	3.42[7]	3.69[7]	1.27	1.08	1.37
3000	1.36[5]	1.93[5]	1.91[9]	2.72[9]	3.04[9]	1.43	1.12	1.59

energy surface based on CCSD(T)/aug-cc-pVTZ data.[43] The direct electronic structure calculations were performed using the MOLPRO[44] suite of quantum chemistry programs. The sampling procedure used in these calculations is similar to that used for CH_4 and involves a set of nested hyperrectangles, which are sampled independently and then weighted by their volumes. The edges of the hyperrectangles were defined by the one coordinate turning points with $E = 13\,000\ \text{cm}^{-1}$.

The minimum energy structure of the vinyl radical, H_2CCH', is a bent Y where the CCH′ angle, θ, is 137°. This causes the potential energy surface to possess two mirror image minima both of which can be accessed via the CCH′ bending motion. Restricting our attention first to this angle we apply our algorithm to sample only along this bend, using either the angular coordinate, θ, or the corresponding Cartesian normal mode representation. The calculated state densities are shown in Fig. 3(a) for the QCSID(T)/MP2 potential with $M = 12\,800$ sampling points. The potentials obtained along the respective coordinates are also shown in Fig. 3(b).

The angular coordinate, θ, is a better one-dimensional description of the motion as can be seen from the comparison of the potential energy curves. Accessing the saddle point at $\theta = 180°$ is not possible in this one-coordinate picture using Cartesian normal modes and would require simultaneous displacements along several normal coordinates, indicating coupling among those coordinates in the fairly low energy regions of the saddle point. The potential curves along neither coordinate are particularly harmonic. The curve along the normal coordinate has a significant quartic component, as evidenced by the drop in the density of states relative to the analytic harmonic solution. Although the angular sampling appears to track the analytic harmonic solution until it reaches the energy of the barrier at $\theta = 180°$, this is a rather fortuitous cancellation of both positive and negative anharmonicities. The region with angles larger than 140° yields a higher density

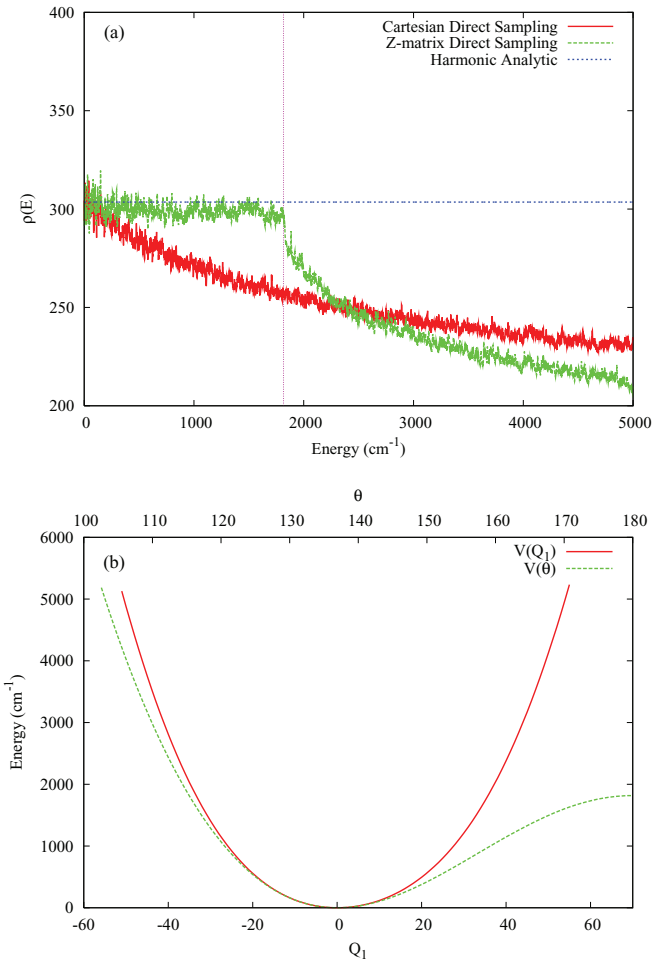

FIG. 3. (a) One-dimensional state density for the H_2C–C–H vibration for two choices of the bending coordinate and the harmonic approximation to it. The energy of the barrier between the two equivalent minima is shown as the pink vertical line. (b) The potential energy curves along two coordinates.

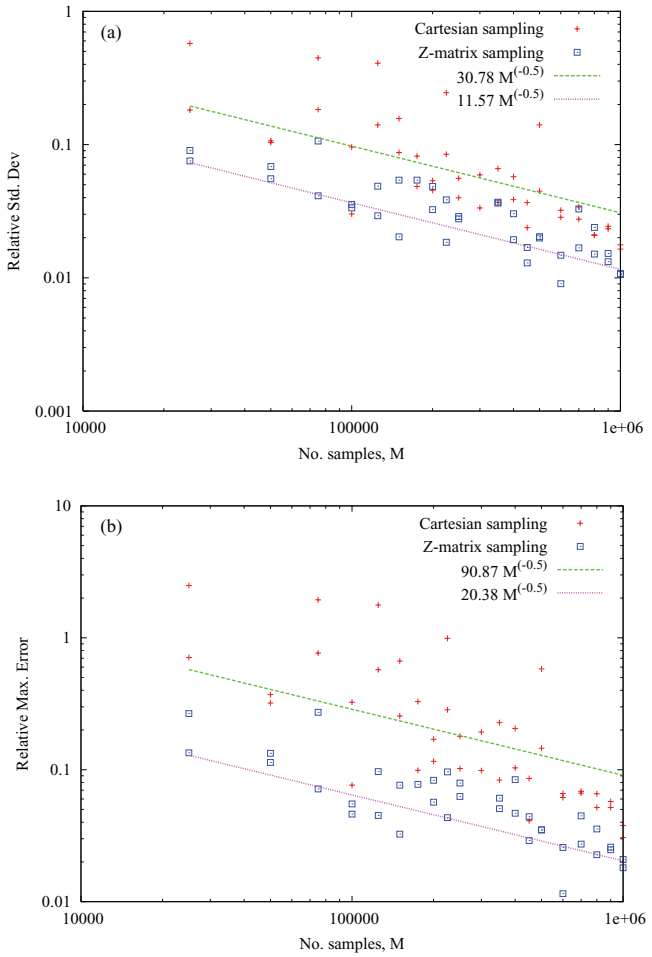

FIG. 4. (a) Relative standard deviation and (b) relative maximum error for W at two energies, 5000 cm^{-1} and 10 000 cm^{-1}, using both coordinate systems. The solid curves are the best fits of the data points to the form $a \cdot M^{-0.5}$.

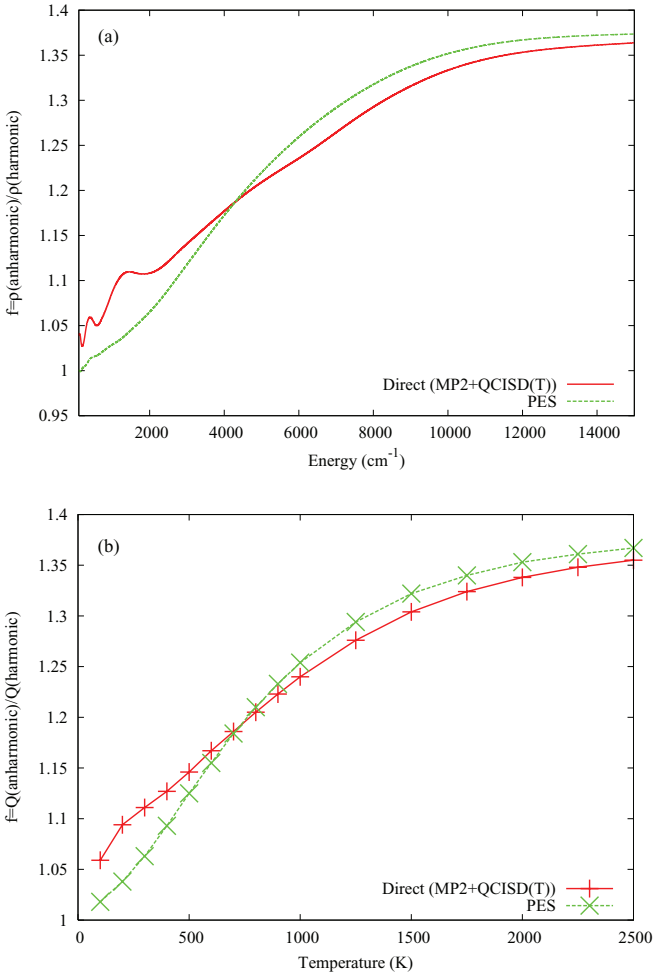

FIG. 5. Anharmonicity corrections to the (a) density of states and (b) partition function for the vinyl radical.

of states than the harmonic potential, while the region with angles smaller than 130° yields a lower density.

In addition to reducing coupling, the use of the angular coordinate can also conveniently enforce the separation of the two equivalent minima, since we can set its maximum value to 180°. This naturally prevents double counting states arising in the two minima. The truncation does not occur naturally using the Cartesian normal mode coordinates, and, with large enough bounds on those coordinates, we would need to divide the density of states by two to obtain the correct result. The possibility of sampling some, but not all, of the states belonging to the other well may result in systematic error to the Cartesian sampling above certain threshold energies. While the truncation of space could also be enforced in the Cartesian coordinate system, it does not appear as a natural consequence of the chosen coordinates as in the curvilinear sampling. An additional advantage is that while the Cartesian normal modes are associated with a particular minimum, the curvilinear coordinates are not and so can more easily sample multiple minima when not identical by symmetry.

To further illustrate the usefulness of curvilinear coordinate sampling, the convergence metrics defined in Sec. III A are shown in Fig. 4. For this test we employed the fitted vinyl potential and performed 20 independent runs for both choices of coordinate system from which we then calculated the standard deviations. Unlike for methane there is a clear efficiency improvement when using curvilinear coordinates. Here we assume $M^{-0.5}$ convergence and fit only the prefactor for the two coordinate choices. Using curvilinear z-matrix coordinates, a relative error in ρ of 3% is obtained with $M = 100\,000$, whereas 10× as many sampled geometries are required using Cartesian normal mode coordinates. This efficiency improvement is attributed in part to the reduced coupling of the CCH′ bend with the other motions, as discussed above.

Next, anharmonic corrections for ρ and Q are calculated for all nine internal coordinates, $M = 2\,457\,600$, and the composite QCISD(T)/MP2 potential. The results are shown in Fig. 5. Using our parallelized code, distributed over 768 processors, this constituted approximately 17 h of walltime. These are compared with a run using the fitted potential and 10 000 000 sampling points. The smaller direct sampling run shows some additional uncertainty in the low energy region because we did not choose to weight this region significantly here. The agreement between the two calculations for ρ is within 2% at the dissociation threshold and is 1.36.

Direct sampling of the potential involves multiple calls to an external electronic structure program yielding numerous inefficiencies in terms of overhead and redundant

computational work. Various schemes to improve the efficiency of such direct sampling approaches have been developed in the context of both Monte Carlo integration and molecular dynamics;[45–47] however, we have not yet implemented any such approach.

IV. CONCLUSIONS

In this paper we have introduced an algorithm for evaluating classical phase space integrals using arbitrary curvilinear or rectilinear coordinate systems via Monte Carlo sampling. This algorithm was used to calculate vibrational state counts, state densities, and partition functions for CH_4 and C_2H_3. The present implementation yields classical values for a range of energies and for zero total angular momentum. With suitable modifications it can be used to calculate rovibrational properties. The calculated values of ρ and Q include the effects of all anharmonicities in the underlying potential energy surface, including single-mode anharmonicity and anharmonic coupling. We have demonstrated that this algorithm can be efficiently used with direct *ab initio* potential evaluations. The use of curvilinear coordinates allows for more convenient coordinate choices, which can lead to more accurate results and faster convergence. This approach may be useful to validate approximate methods, suitable for application to larger systems. For example, it can be used to test models for separability and the optimality of coordinate systems. While these effects have been considered previously,[48,49] the present approach can provide tests of these methods.

ACKNOWLEDGMENTS

Financial support from the Division of Chemical Sciences, Geosciences, and Biosciences, Office of Basic Energy Sciences, U.S. Department of Energy (Grant No. DE-AC04-94-AL85000) is gratefully acknowledged.

[1] D. I. Lyakh, M. Musial, V. F. Lotrich, and R. J. Bartlett, Chem. Rev. **112**, 182 (2012).
[2] A. W. Jasper and N. Hansen, Proc. Combust. Inst. **34**, 279 (2013).
[3] R. G. Gilbert and S. C. Smith, *Theory of Unimolecular and Recombination Reactions* (Blackwell Scientific, Boston, 1990).
[4] T. Baer and W. L. Hase, *Unimolecular Reaction Dynamics: Theory and Experiments* (Oxford University Press, New York, 1996).
[5] S. J. Klippenstein, in *Comprehensive Chemical Kinetics* (Elsevier, 2003), Vol. 39, p. 55.
[6] T. Beyer and D. F. Swinehart, Commun. ACM **16**, 379 (1973).
[7] S. E. Stein and B. S. Rabinovitch, J. Chem. Phys. **58**, 2438 (1973).
[8] K. S. Pitzer and W. D. Gwinn, J. Chem. Phys. **10**, 428 (1942).
[9] J. Zheng, T. Yu, E. Papajak, I. M. Alecu, S. L. Mielke, and D. G. Truhlar, Phys. Chem. Chem. Phys. **13**, 10885 (2011).
[10] V. A. Lynch, S. L. Mielke, and D. G. Truhlar, J. Phys. Chem. A **109**, 10092 (2005).
[11] S. Chempath, C. Predescu, and A. T. Bell, J. Chem. Phys. **124**, 234101 (2006).
[12] J. M. Bowman, T. Carrington, and H.-D. Meyer, Mol. Phys. **106**, 2145 (2008).
[13] C. Xu, B. Jiang, D. Xie, S. C. Farantos, S. Y. Lin, and H. Guo, J. Phys. Chem. A **111**, 10353 (2007).
[14] R. Chen, G. Ma, and H. Guo, J. Chem. Phys. **114**, 4763 (2001).
[15] R. Siebert, P. Fleurat-Lessard, R. Schinke, M. Bittererova, and S. C. Farantos, J. Chem. Phys. **116**, 9749 (2002).
[16] M. Basire, P. Parneix, and F. Calvo, J. Chem. Phys. **129**, 081101 (2008).
[17] T. L. Nguyen and J. R. Barker, J. Phys. Chem. A **114**, 3718 (2010).
[18] J. Troe and V. G. Ushakov, J. Phys. Chem. A **113**, 3940 (2009).
[19] S. Schmatz, Chem. Phys. **346**, 198 (2008).
[20] M. Berblinger and C. Schlier, J. Chem. Phys. **96**, 6834 (1992).
[21] M. Berblinger, C. Schlier, J. Tennyson, and S. Miller, J. Chem. Phys. **96**, 6842 (1992).
[22] G. Taubmann and S. Schmatz, Phys. Chem. Chem. Phys. **3**, 2296 (2001).
[23] J. R. Barker, J. Phys. Chem. **91**, 3849 (1987).
[24] J. D. Doll, Chem. Phys. Lett. **72**, 139 (1980).
[25] R. Viswanathan, L. M. Raff, and D. L. Thompson, J. Chem. Phys. **81**, 828 (1984).
[26] M. Berblinger and C. Schlier, J. Chem. Phys. **101**, 4750 (1994).
[27] G. Z. Whitten and B. S. Rabinovich, J. Chem. Phys. **38**, 2466 (1963).
[28] J. Gang, M. J. Pilling, and S. H. Robertson, J. Chem. Soc., Faraday Trans. **92**, 3509 (1996).
[29] S. L. Mielke and D. G. Truhlar, J. Chem. Phys. **115**, 652 (2001).
[30] T. F. Miller III and D. C. Clary, J. Chem. Phys. **119**, 68 (2003).
[31] S. L. Mielke and D. G. Truhlar, J. Phys. Chem. A **113**, 4817 (2009).
[32] K. Yagi, M. Keçeli, and S. Hirata, J. Chem. Phys. **137**, 204118 (2012).
[33] B. Njegic and M. S. Gordon, J. Chem. Phys. **125**, 224102 (2006).
[34] D. Strobusch and C. Scheurer, J. Chem. Phys. **135**, 124102 (2011).
[35] D. Lauvergnat and A. Nauts, J. Chem. Phys. **116**, 8560 (2002).
[36] M. A. Harthcock and J. Laane, J. Phys. Chem. **89**, 4231 (1985).
[37] Y. Wang and C. H. Mak, Chem. Phys. Lett. **235**, 37 (1995).
[38] See comp.chem.umn.edu/tbpac for TB, version 1.0.1 written by T. Liu and D. G. Truhlar, University of Minnesota, 2004.
[39] A. Chakraborty, D. G. Truhlar, J. M. Bowman, and S. Carter, J. Chem. Phys. **121**, 2071 (2004).
[40] J. Troe, J. Chem. Phys. **66**, 4745 (1977).
[41] J. Troe, J. Chem. Phys. **66**, 4758 (1977).
[42] A. W. Jasper and J. A. Miller, J. Phys. Chem. A **115**, 6438 (2011).
[43] A. R. Sharma, B. J. Braams, S. Carter, B. C. Shepler, and J. M. Bowman, J. Chem. Phys. **130**, 174301 (2009).
[44] H.-J. Werner, P. J. Knowles, F. R. Manby, M. Schütz *et al.*, MOLPRO, version 2010.1, a package of *ab initio* programs, 2010, see http://www.molpro.net.
[45] R. P. Steele, M. Head-Gordon, and J. C. Tully, J. Phys. Chem. A **114**, 11853 (2010).
[46] T. Atsumi and H. Nakai, Chem. Phys. Lett. **490**, 102 (2010).
[47] R. P. Steele and J. C. Tully, J. Chem. Phys. **135**, 184107 (2011).
[48] B. M. Wong and W. H. Green, Mol. Phys. **103**, 1027 (2005).
[49] D. P. Tew, N. C. Handy, and S. Carter, J. Chem. Phys. **125**, 084313 (2006).